



Mono-oxime bisquaternary acetylcholinesterase reactivators with prop-1,3-diyl linkage—Preparation, in vitro screening and molecular docking

Kamil Musilek^{a,c,*}, Marketa Komloova^b, Ondrej Holas^b, Anna Horova^a, Miroslav Pohanka^d, Frank Gunn-Moore^e, Vlastimil Dohnal^c, Martin Dolezal^b, Kamil Kuca^{c,d}

^a University of Defence, Faculty of Military Health Sciences, Department of Toxicology, Trebesska 1575, 500 01 Hradec Kralove, Czech Republic

^b Charles University, Faculty of Pharmacy, Department of Pharmaceutical Chemistry and Drug Control, Heyrovského 1203, 500 05 Hradec Kralove, Czech Republic

^c University of Jan Evangelista Purkyně, Faculty of Science, Department of Chemistry, Ceske mladeze 8, 400 96 Usti nad Labem, Czech Republic

^d University of Defence, Faculty of Military Health Sciences, Centre of Advanced Studies, Trebesska 1575, 500 01 Hradec Kralove, Czech Republic

^e School of Biology, University of St. Andrews, Medical and Biological Sciences Building, St. Andrews, KY16 9TF Fife, UK

ARTICLE INFO

Article history:

Received 30 June 2010

Revised 5 December 2010

Accepted 7 December 2010

Available online 16 December 2010

Keywords:

Acetylcholinesterase

Organophosphate

Reactivation

Oxime

In vitro

Docking

ABSTRACT

The treatment of organophosphorus (OP) poisoning consists of the administration of a parasympatholytic agent (e.g., atropine), an anticonvulsant (e.g., diazepam) and an acetylcholinesterase (AChE) reactivator (e.g., obidoxime). The AChE reactivator is the causal treatment of OP exposure, because it cleaves the OP moiety covalently bound to the AChE active site. In this paper, fourteen novel AChE reactivators are described. Their design originated from a former promising compound K027. These compounds were synthesized, evaluated in vitro on human AChE (hAChE) inhibited by tabun, paraoxon, methylparaoxon and DFP and then compared to commercial hAChE reactivators (pralidoxime, HI-6, trimedoxime, obidoxime, methoxime) or previously prepared compounds (K027, K203). Three of these novel compounds showed a promising ability to reactivate hAChE comparable or better than the used standards. Consequently, a molecular docking study was performed for three of these promising novel compounds. The docking results confirmed the apparent influence of π - π or cation- π interactions and hydrogen bonding for reactivator binding within the hAChE active site cleft. The SAR features concerning the non-oxime part of the reactivator molecule are also discussed.

© 2010 Elsevier Ltd. All rights reserved.

1. Introduction

Acetylcholinesterase (EC 3.1.1.7; AChE) is an essential enzyme in the human body for the degradation of acetylcholine and the termination of neurotransmission. This enzyme can be inhibited by many natural or artificial compounds. Among artificial compounds that are able to inhibit AChE, the organophosphorus agents (OP; e.g., nerve agents, pesticides, industrial agents) are some of the most dangerous compounds developed by man.¹ Nerve agents (e.g., sarin, soman, tabun—GA, VX; Fig. 1), OP pesticides (e.g., paraoxon—POX, methylparaoxon—MePOX) or mimic agents (e.g., DFP) irreversibly inhibit the AChE active site, specifically amino acid residue S203 (human AChE; hAChE) within the hAChE active site.² Furthermore, they may be degraded and coordinated within the hAChE active site interacting with other amino acid residues (Phe338, His447). This process is termed ‘aging’.³ Their overall effect results in irreversible hAChE inhibition and subsequent permanent neuronal stimulation. Such constant stimulation leads firstly to muscarinic (e.g., miosis, salivation, lacrimation) or nicotinic induced symptoms (e.g.,

muscular fasciculation). Consequently, a cholinergic crisis (overstimulation of cholinergic receptors) with central nervous presenting symptoms occur with further depression of the breathing center in the medulla oblongata and the breathing muscles which may result in death for the organism.⁴

OP intoxication can be managed via two general strategies. The pre-treatment strategy is based on using a prophylactic drug prior to OP intoxication.⁵ Reversible AChE inhibitors (e.g., pyridostigmine, galanthamine), oxime reactivators (e.g., HI-6) or bioscavengers (e.g., recombinant butyrylcholinesterase, paraoxonase) can be used to protect hAChE from the binding of the OP moiety.⁶ A post-treatment strategy is managed after OP intoxication. This method consist of the administration of a parasympatholytic agent (e.g., atropine), an oxime reactivator (e.g., pralidoxime, HI-6, obidoxime, trimedoxime, methoxime, Hlo-7, Ortho-7; 1–5; Fig. 2) and an anticonvulsant (e.g., diazepam).⁷ Whereas the parasympatholytic agents and anticonvulsants are used as symptomatic treatments, the oxime reactivators attempt to tackle directly the causes of the OP intoxication. The nucleophilic oxime moiety is able to cleave the OP bound to Ser203 (in hAChE) and restore hAChE's vital function.⁴ The limitation of an oxime function is the inability to reactivate an aged enzyme.⁸ Additionally, no one

* Corresponding author. Tel.: +420 973 251 523; fax: +420 495 518 094.

E-mail address: kamil.musilek@gmail.com (K. Musilek).

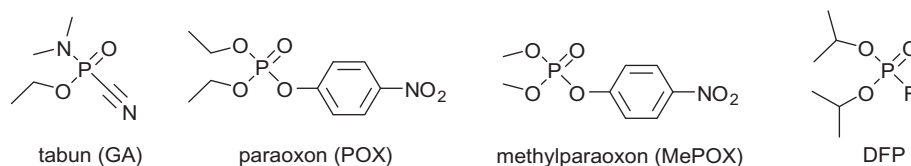


Figure 1. Representative images of the organophosphorus compounds used in this study.

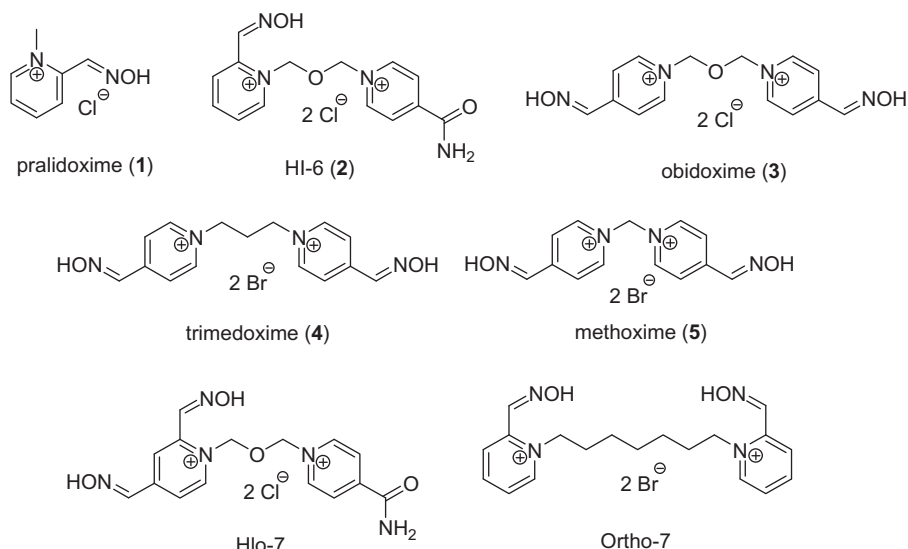


Figure 2. Commercially available and promising hAChE reactivators.

oxime is able to reactivate structural different OP moieties. Thus, the structure of the oxime reactivator determines its ability to restore function of hAChE inhibited by different OP moieties.⁹

Formerly, the compound HI-6 was considered to be most broad spectrum reactivator against nerve agent intoxication.¹⁰ Hence, its large scale production is already in progress in several countries worldwide.¹¹ However, it is not able to manage effectively GA-intoxication.¹² Additionally, it was found to be a poor reactivator of OP pesticide intoxication.¹² Thus, there is a need for an effective hAChE reactivator for both GA and OP pesticide poisoning.

2. Design and synthesis mono-oxime bispyridinium reactivators

Mono-oxime bispyridinium compounds are developed in this paper. Their design originated from structural findings (SAR) from formerly determined reactivators of hAChE which had been inhibited by GA and OP pesticides. GA-inhibited hAChE became a focus of interest due to its difficult reactivation by some commercial oximes (1 and 2); although these oximes (1 and 2) were able to reactivate sufficiently other nerve agent poisonings (e.g., sarin, cyclosarin, VX).¹⁰ In addition, the OP pesticides were shown to be insufficiently reactivated by some of the commercially available

compounds (1 and 2), which are currently used globally (1) to treat OP pesticide intoxication.¹³

The main aim of this paper was to extend our previous structural findings on OP reactivation.⁹ Namely, several compounds were previously described as promising oximes for the reactivation of OP pesticide inhibited hAChE.¹⁴ Among them, compound K027 (6; Fig. 3) was found to be a potent reactivator with a valuable activity/toxicity profile.¹⁵ Moreover, the in vitro results of compound 6 were further confirmed by in vivo experiments.¹⁶ Several other compounds were also described as being potential promising oximes for the reactivation of GA-inhibited hAChE.¹⁷ From these hAChE reactivators, compound K203 (7; Fig. 3) showed the best results against GA-inhibited hAChE compared to commercially available compounds (1–5), again providing a valuable activity/toxicity profile.¹⁸ The superior reactivation of GA-inhibited hAChE by compound 7 was again confirmed by in vivo results.^{19–21}

Consequently, novel hAChE reactivators were designed with respect to our previous results which were on compounds 6 and 7 (Fig. 4). The bispyridinium nature of the molecule remained consistent. One oxime moiety in the 4-position, which is essential for reactivation, was also retained. Similarly, the prop-1,3-diyl linkage was used in compound 6, where linkers analogous to 3–4 C–C bonds were found to be the most promising for GA or OP pesticide

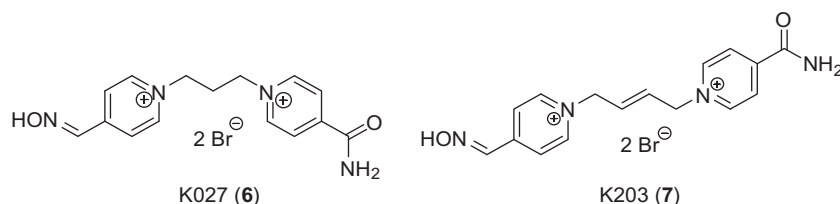


Figure 3. Previously developed reactivators against tabun and OP pesticides induced inhibition of hAChE activity.

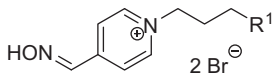
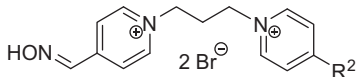
Compound	R ¹	Compound	R ²
			
8	1-pyridinium	12	Me
9	1-pyridazinium	13	<i>tert.</i> -butyl
10	1-quinolinium	14	phenyl
11	1-isoquinolinium	15	CH ₂ OH
		16	COMe
		17	COOH
		18	COOEt
		19	CN
		20	C(NH ₂)=NOH
		21	3,4-CONH ₂

Figure 4. Structure of the newly prepared mono-oxime reactivators.

reactivation.^{22–25} The non-oxime pyridinium ring was substituted in 4-position (**12–21**) by various moieties of different hydrophilic (e.g., hydroxymethyl, carboxyl, nitrile) or hydrophobic (e.g., methyl, *tert*-butyl, phenyl) nature or replaced by a hetero-aromatic ring (**8–11**; e.g., pyridazinium, quinolinium, isoquinolinium) as it was formerly used for analogs of compound **7**.²⁶ These moieties were introduced to establish the possible interactions within the hAChE active site with an emphasis on π - π , π -cationic or other interactions.²⁷

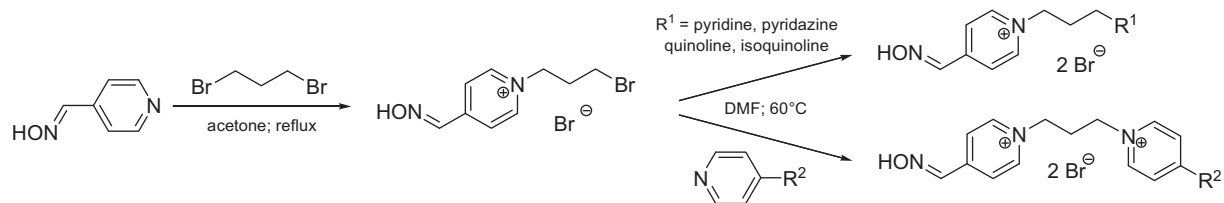
The mono-oxime reactivators with a prop-1,3-diyl linker were prepared via a two step synthesis (Scheme 1). Firstly, the mono-quaternary compound was synthesized in 5 M excess of alkylating agent. The monoquaternary compound was separated from side bisquaternary products by re-crystallization from acetonitrile (MeCN), where the bisquaternary product was almost insoluble. Secondly, this reactivator was completed by the addition of a corresponding heterocyclic derivative (1.5 M excess). The re-crystallization from MeCN was used again to obtain the non-soluble bisquaternary product (**8–21**) with a satisfactory yield and purity.²⁸

3. hAChE reactivation results

The reactivation of recombinant hAChE inhibited by either GA, POX, MePOX or DFP was measured by a standard protocol developed by Ellman.²⁹ GA was chosen as a nerve agent inhibitor of hAChE about which the ability to reactivate hAChE was known.⁸ The selected OP pesticides (POX, MePOX) and a mimic agent (DFP) were chosen for testing as they are appropriately molecular divergent members of the OP family regarding their hAChE inhibition, that is, dimethyl- (MePOX), diethyl- (POX) or diisopropyl- (DFP) moieties. The reactivation results are listed in Table 1.

The reactivation of GA-inhibited hAChE by commercial reactivators (**1–5**) was previously found to be difficult.³⁰ Among them, the use of compounds **1** (3%), **2** (1%) and **5** (3%) resulted as being inappropriate reactivators of GA in vitro at 100 μ M. Compounds **3** (15%) and **4** (31%) showed an ability to reactivate GA, whereas compound **4** (17%) was found to be the best reactivator for GA-inhibited hAChE among commercially available compounds (**1–5**) at a screening concentration of 10 μ M which is relevant for in vivo use.³¹ The previously prepared hAChE reactivators (**6** and **7**) showed different abilities. Though compound **6** (15%) was a poorer reactivator compared to the commercial compound **4** (48%) and was a similar reactivator when compared to its bis-oxime analog **3** (15%) at 100 μ M, compound **7** displayed the best reactivation ability (48% and 21%) against GA-inhibited hAChE at both screening concentrations among all tested compounds. Compound **7** was also previously highlighted as being a promising reactivator of GA-inhibited AChE both in vitro and in vivo.¹⁵ With respect to the newly prepared compounds (**8–21**) and their reactivation ability against GA induced hAChE inhibition, these can be divided in two groups. The first group (**8–13**, **15**, **17–21**) produced a minor reactivation of GA-inhibited hAChE; however this was below 10% which is considered to be the lowest level for a plausible reactivation in vivo.⁴ The second group of compounds **14** (11%) and **16** (12%) showed a reactivation ability comparable to the commercial compound **3** (8%) at 10 μ M, but lower than the commercial compound **4** (17%) or the previously prepared compound **7** (21%). Therefore, compound **7** was considered to be our leading oxime for its reactivation capability against GA induced inhibition.²¹

With regard to POX induced inhibition of hAChE, some of the commercially available compounds **1** (2%), **2** (2%) and **5** (13%) were inefficient reactivators at 10 μ M. However, commercial compounds **3** (22%) and **4** (22%) were found to be potent POX-reactivators with a



Scheme 1. Preparation of mono-oxime reactivators with prop-1,3-diyl linkage.

Table 1

Reactivation data of commercial, previously prepared, and novel hAChE reactivators

Inhibitor Reactivator	GA		POX		MePOX		DFP	
	100 μ M	10 μ M	100 μ M	10 μ M	100 μ M	10 μ M	100 μ M	10 μ M
1	3.3 \pm 0.5	2.4 \pm 0.2	10.7 \pm 0.3	2.1 \pm 0.1	30.2 \pm 0.3	22.4 \pm 0.7	1.3 \pm 0.6	0.1 \pm 0.4
2	0.9 \pm 0.6	0.8 \pm 0.3	6.2 \pm 0.6	1.7 \pm 0.1	13.6 \pm 0.2	17.9 \pm 0.4	0.7 \pm 0.1	1.4 \pm 0.1
3	15.1 \pm 0.9	7.9 \pm 0.5	59.7 \pm 1.0	22.4 \pm 0.4	61.7 \pm 0.3	45.3 \pm 0.9	7.6 \pm 0.7	3.3 \pm 0.4
4	31.5 \pm 1.2	16.9 \pm 0.2	44.3 \pm 0.6	22.5 \pm 1.3	51.4 \pm 0.9	59.5 \pm 0.7	10.0 \pm 0.5	2.7 \pm 0.3
5	2.9 \pm 0.01	2.1 \pm 0.5	16.1 \pm 0.5	1.8 \pm 0.3	14.2 \pm 0.1	14.3 \pm 0.2	2.4 \pm 0.1	0.6 \pm 0.3
6	15.2 \pm 0.6	7.8 \pm 0.5	48.0 \pm 0.5	20.8 \pm 1.0	55.6 \pm 0.7	33.9 \pm 0.3	5.7 \pm 0.3	2.1 \pm 0.1
7	48.1 \pm 1.5	21.2 \pm 0.3	39.3 \pm 0.4	13.1 \pm 0.4	55.9 \pm 0.5	41.1 \pm 0.1	4.4 \pm 0.1	2.1 \pm 0.4
8	5.3 \pm 0.3	4.4 \pm 0.2	28.4 \pm 4.9	13.0 \pm 0.7	9.3 \pm 0.6	6.0 \pm 0.7	6.4 \pm 0.2	1.7 \pm 0.1
9	5.3 \pm 0.3	4.5 \pm 0.3	26.0 \pm 0.2	18.8 \pm 1.1	8.8 \pm 1.0	6.6 \pm 0.8	1.2 \pm 0.1	16.8 \pm 0.4
10	0.6 \pm 0.1	2.6 \pm 0.3	5.1 \pm 0.9	7.5 \pm 0.3	8.3 \pm 1.5	9.5 \pm 0.7	0.8 \pm 0.4	1.2 \pm 0.2
11	3.0 \pm 0.1	4.2 \pm 0.5	4.6 \pm 0.3	6.7 \pm 0.3	18.5 \pm 0.6	7.9 \pm 0.2	0.6 \pm 0.2	0.8 \pm 0.3
12	3.8 \pm 0.1	3.3 \pm 0.4	15.9 \pm 0.8	23.8 \pm 0.4	14.3 \pm 1.0	4.6 \pm 0.1	13.1 \pm 0.4	11.1 \pm 0.6
13	3.4 \pm 0.4	5.3 \pm 0.3	16.7 \pm 0.7	0.6 \pm 0.3	6.8 \pm 0.6	4.9 \pm 0.9	1.1 \pm 0.3	0.1 \pm 0.3
14	10.1 \pm 0.4	11.2 \pm 0.5	23.2 \pm 1.1	21.0 \pm 0.9	31.6 \pm 1.8	16.6 \pm 1.2	3.9 \pm 0.3	2.3 \pm 0.1
15	1.8 \pm 0.2	3.6 \pm 0.3	13.7 \pm 0.3	7.6 \pm 0.1	11.3 \pm 0.1	3.5 \pm 0.2	1.8 \pm 0.2	0.7 \pm 0.5
16	12.1 \pm 0.8	12.9 \pm 0.4	55.2 \pm 0.9	13.3 \pm 0.7	10.7 \pm 0.3	31.2 \pm 0.1	1.8 \pm 0.1	0.1 \pm 0.1
17	9.1 \pm 0.5	4.2 \pm 0.01	17.0 \pm 1.0	30.7 \pm 0.3	7.5 \pm 0.8	3.1 \pm 0.2	6.2 \pm 0.8	1.4 \pm 0.2
18	8.8 \pm 0.3	8.2 \pm 0.2	51.4 \pm 2.0	20.2 \pm 0.5	15.3 \pm 0.7	28.1 \pm 0.3	1.9 \pm 0.2	1.3 \pm 0.3
19	6.2 \pm 0.9	5.9 \pm 0.9	15.8 \pm 0.5	23.4 \pm 1.9	24.2 \pm 0.9	4.0 \pm 0.7	12.7 \pm 0.1	7.4 \pm 0.1
20	9.6 \pm 0.2	8.9 \pm 0.6	72.2 \pm 1.4	38.9 \pm 0.8	37.2 \pm 0.4	52.2 \pm 0.4	3.1 \pm 0.1	1.3 \pm 0.2
21	5.4 \pm 0.5	4.4 \pm 0.2	9.9 \pm 0.2	29.0 \pm 0.5	10.3 \pm 0.4	2.6 \pm 0.5	0.6 \pm 0.3	0.3 \pm 0.2

%, mean value of three independent determinations \pm SD on recombinant hAChE; time of reactivation by AChE reactivators 15 min; pH 7.4; temperature 25 °C.

similar capability at a concentration of 10 μ M, which would be attainable during an in vivo administration. The previously prepared compounds **6** (48%) and **7** (39%) showed a comparable or lower reactivation ability towards POX-inhibited hAChE at 100 μ M when compared to compounds **3** (60%) or **4** (44%), whereas compound **6** (21%) resulted with a slightly less reactivation capability than compounds **3** and **4** (both 22%) at 10 μ M concentration. The newly prepared mono-oximes (**8–21**) displayed a variety of reactivation capabilities against POX induced inhibition. Five compounds **12** (24%), **17** (31%), **19** (23%), **20** (39%) and **21** (29%) were found to be better POX-reactivators than commercially available compounds **3** and **4** (both 22%) at 10 μ M. Among them, compound **20** (39%) was the best reactivator of POX-inhibited hAChE with almost double the reactivation ability compared to the standard compounds **3** and **4** at 10 μ M, which makes compound **20** particularly interesting for further testing.

For MePOX-inhibited hAChE, several commercial compounds **1** (22%), **2** (18%), **5** (41%) showed again a poorer reactivation ability compared to compounds **3** (45%) and **4** (60%) at 10 μ M. Namely, compound **4** (60%) retained a high reactivation ability at a 10 μ M concentration which highlights the potential use of this bis-oxime against MePOX inhibition instead of other commercial oximes. The previously prepared compounds **6** (34%) and **7** (41%) showed promising reactivation of MePOX induced inhibition, but their reactivation abilities were lower than the commercially available oximes **3** (45%) and **4** (60%) at 10 μ M. The newly prepared mono-oximes (**8–21**) displayed various abilities for the reactivation of MePOX-inhibited hAChE. Four of them **14** (17%), **16** (31%), **18** (28%) and **20** (52%) were able to exceed 10% reactivation at 10 μ M concentration. From these, compound **20** (52%) displayed a promising reactivation ability against MePOX slightly lower than the commercial compound **4** (60%) at concentration of 10 μ M. Thus, compound **20** appears to be a relevant candidate for further in vivo evaluation against MePOX and POX-inhibited hAChE.

The commercial oximes (**1–5**) were known to be poor reactivators of DFP-inhibited hAChE. Our in vitro evaluation confirmed this finding, where only compound **4** (10%) was able to attain 10% reactivation at 100 μ M. The previously prepared compounds **6** (6%) and **7** (4%) also followed this trend with only a minor reactivation of DFP induced inhibition. However, notably several newly prepared mono-oximes (**8–21**) showed some reactivation ability against DFP induced inhibition. Two newly prepared compounds **12**

(13%) and **19** (13%) were able to exceed 10% reactivation at a concentration of 100 μ M and two compounds **9** (17%) and **12** (11%) at a concentration of 10 μ M. This highlighted compound **12** as suitable for further studies against DFP-inhibited hAChE.

In this study, some compounds (e.g., **2**, **4**, **16–17**, **19–21**) were found to have better reactivation ability at a lower concentration (10 μ M) than at a higher concentration (100 μ M). These results may be explained by mixed reactivation-inhibition properties of hAChE reactivators at these screened concentrations.^{32,33} Thus, the inhibition data (IC_{50}) were determined for the main compounds of interest (**1–7**, **14**, **16** and **20**; Table 2).²⁹ Compound **16** (IC_{50} 105 μ M) was the best inhibitor among these oximes. Confirming our hypothesis, compound **16** resulted as a poorer reactivator of MePOX inhibited hAChE at a concentration of 100 μ M (11%) than 10 μ M (31%), because it produced directly 50% hAChE inhibition at the 100 μ M concentration (screening concentration 100 μ M \approx IC_{50} 105 μ M). At 10 μ M, compound **16** was a better reactivator (31%) because its inhibition ability was decreased 10-fold, but would not affect reactivation. Similar results were obtained for compounds **2** (IC_{50} 203 μ M \approx 25% hAChE inhibition at 100 μ M), **4** (IC_{50} 167 μ M \approx 30% hAChE inhibition at 100 μ M) and **20** (IC_{50} 291 μ M \approx 17% hAChE inhibition at 100 μ M). All these reactivators (**2**, **4**, **16** and **20**) were hypothesized to work via this described mixed reactivation-inhibition mechanism.

The activity/toxicity profile of hAChE reactivator is other important factor for its further use. The less toxic compounds, but the least active in case of GA inhibition, are commercial reactivators

Table 2 IC_{50} data of selected hAChE reactivators

Reactivator	hAChE $IC_{50} \pm$ SD (μ M)
1	878 \pm 171
2	203 \pm 39
3	577 \pm 113
4	167 \pm 33
5	2010 \pm 391
6	711 \pm 139
7	566 \pm 110
14	112 \pm 22
16	105 \pm 20
20	291 \pm 56

1 (LD₅₀ mice 264 mg/kg), **2** (671 mg/kg), **5** (642 mg/kg) and the known reactivator **6** (673 mg/kg).^{16,27} The compounds with improved reactivation ability towards GA resulted as reactivators with slightly elevated toxicity—**3** (188 mg/kg), **4** (151 mg/kg) and **7** (95 mg/kg).²⁷ The novel compounds were prepared with the idea of increased reactivation ability and intermediate toxicity (higher toxicity to compound **6**, but lower to compound **7**), but their toxicity were not yet evaluated and will be aim of further experiments.

4. Molecular docking results and SAR discussion

Molecular docking studies were performed on compound **6**, **14**, **16** and **20** in order to rationalize their possible interactions with GA-inhibited hAChE.³⁴ Compound **6** was selected as the key structure used for the design of all the novel reactivator series of compounds. Additionally, compounds **14**, **16** and **20** were used as promising reactivators of GA-inhibited hAChE, as well as being promising reactivators of POX- and MePOX-inhibited hAChE (Table 1). Though they were found to be poorer reactivators of GA-inhibited hAChE when compared to the previously prepared compounds **6** and **7**, their spatial orientation in the AChE active site might help in further structure-based design of hAChE reactivators.

Three crystal structures of GA-conjugated AChE were used for the docking calculations (GA-hAChE–1b41—crystal structure of hAChE in complex with fasciculin 2, GA-mAChE–2jez, 2jfo). The structure 1b41 was chosen as an example of native hAChE with a good structural resolution (2.76 Å), where the GA structure was manually added to the active site residue Ser203 and the whole molecule was minimized using Autodock Tools.³⁵ The structures 2jez (with Hlo-7; resolution 2.60 Å) and 2jfo (with Ortho-7; 2.50 Å) were chosen as tabun-conjugated enzymes that produced better results for docking-in vitro data correlation than structures without an OP moiety.³⁶ In contrast to molecular docking of hAChE inhibitors (e.g., those used in the treatment of Alzheimer's disease), the OP covalently binds the serine residue within the active site, and changes the amino acid residues interactions, decreasing the space available for an AChE reactivator.³⁷ Thus, the structures with non-bonded OP moiety were not used for molecular docking analysis. Of note, other structures might also be used (e.g., 2wu3, 2gyw, 2whr, 2x8b, 3lii).^{37–41}

Not surprisingly, the best scoring results were obtained for crystal structure 2jez of GA-inhibited mAChE containing oxime Hlo-7, because the structure of Hlo-7 molecule is a very similar to chosen and docked newly prepared compounds. The oxime-linked aromatic ring of compound **6** (the lowest binding energy –10.28 kcal/mol) displayed cation- π interactions with three aromatic residues (Tyr337, Phe338 and Tyr341) of internal anionic site (IAS; Fig. 5).⁴² The second aromatic ring with a carbamoyl moiety was sandwiched among 4 aromatic residues (Tyr72, Tyr124, Trp286 and Phe297) with a peripheral anionic site (PAS).⁴² The carbamoyl moiety was able to interact with Glu285 (3.2 Å), Ser298 (2.0 Å) and one water molecule (2.1 Å). Compound **14** (the lowest binding energy –8.31 kcal/mol) showed a different kind of interaction with mAChE. Its oxime-linked aromatic ring displayed cation- π interactions with two aromatic residues (Phe338 and Tyr341) and one T-stacking with PAS (Trp286). The second aromatic ring with phenyl moiety was T-stacked to PAS (Trp286) and the phenyl moiety was found close to His287. Compound **16** (the lowest binding energy –7.19 kcal/mol) resulted in a similar top-scored docking pose to compound **14**. Its oxime-linked aromatic ring was stabilized by cation- π interactions (Phe297, Phe338 and Tyr341) in the IAS. The aromatic ring with methylcarbonyl moiety was T-stacked to PAS (Trp286), whereas the methylcarbonyl moiety displayed a hydrogen bond with Ser293. Similarly as with compound

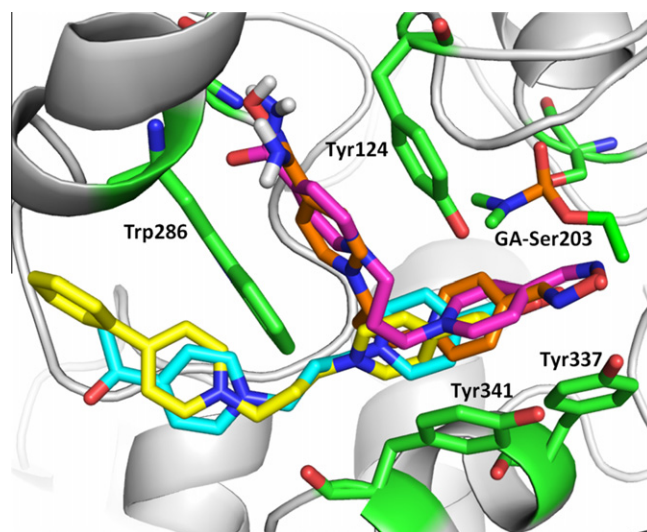


Figure 5. Top-scored docking poses of compounds **6** (magenta), **14** (yellow), **16** (blue) and **20** (orange).

6, the oxime-linked aromatic ring of compound **20** (the lowest binding energy –10.26 kcal/mol) was stabilized by cation- π interactions (Tyr337, Phe338 and Tyr341) within the IAS. The aromatic ring containing an amidoxime moiety was sandwiched among the PAS residues (Tyr72, Tyr124, Trp286 and Phe297). The amidoxime moiety showed hydrogen bonding with residues Glu285, Ser298 and one water molecule similar to that of the carbamoyl moiety of compound **6**.

Regarding the SAR of hAChE reactivators for GA or OP pesticide inhibited hAChE, several important features have to be considered.⁹ Firstly, the mono-oxime compounds were already determined as sufficient reactivators based on the pK_a of the oxime moiety.⁴³ The 4-position of the oxime moiety on the pyridinium ring was previously found to be optimal.⁴⁴ Secondly, the connecting linker between pyridinium rings analogous to 3 or 4 carbon-carbon bonds was also previously described as a valuable molecular feature.⁹ In addition, the non-oxime part of the reactivator molecule may influence its binding to the enzyme as well as its tissue penetration and ionization. Importantly, the second pyridinium ring (**8**) is a key factor for cation- π interactions with aromatic amino acid residues from the PAS as the cation- π interaction is the strongest non-covalent interaction.^{45–47} Its modification by other hydrophobic moieties (e.g., **14**-phenyl) led to an increase in reactivation capability (Table 1). A plausible explanation of this reactivation increase is the presence of additional π - π interactions and thereby providing strong binding within AChE active site. In contrast, the hydrophilic moieties on the non-oxime pyridinium ring (e.g., **16**-methylcarbonyl, **20**-amidoxime) also showed an increase in its reactivation ability. This finding may be explained by the setting up of important hydrogen bonds between the enzyme's amino acid residues and reactivator's hydrophilic moieties. The development of the non-oxime part of the hAChE reactivator based on a combination of both hydrophobic and hydrophilic molecular properties will require future investigations.

5. Conclusion

The mono-oxime bisquaternary hAChE reactivators were designed to be analogs of a former promising compound K027. Fourteen novel compounds were synthesized and evaluated by an in vitro model for GA, POX, MePOX and DFP-induced inhibition of hAChE activity. The reactivation capability of these new

compounds was compared to commercially available compounds and the previously produced compounds. Three of the novel compounds provided promising in vitro results which were as good as or better than the known reactivators. These three compounds were further subjected to molecular docking studies which showed apparent interactions within the hAChE active site. Namely, π – π or cation– π interactions and hydrogen bonding were all highlighted as key factors influencing reactivation. In addition some physical–chemical properties were calculated and the valuable SAR features were predicted.

6. Experimental section

6.1. Chemical preparation

Solvents (acetone, DMF, MeCN) and reagents were purchased from Fluka and Sigma–Aldrich (Prague, Czech Republic) and used without further purification. Reactions were monitored by TLC using DC-Alufolien Cellulose F (Merck, Darmstadt, Germany) and mobile phase BuOH/CH₃COOH/H₂O 5:1:2, detection by solution of Dragendorff reagent (solution containing 10 mL CH₃COOH, 50 mL H₂O and 5 mL of basic solution prepared by mixing of two fractions—fraction A: 850 mg Bi(NO₃)₃, 40 mL H₂O, 10 mL CH₃COOH; fraction B: 8 g KI, 20 mL H₂O). Melting points were measured on micro heating stage PHMK 05 (VEB Kombinat Nagema, Radebeul, Germany) and were uncorrected.

NMR spectra were generally recorded at Varian Gemini 300 (¹H 300 MHz, ¹³C 75 MHz, Palo Alto CA, USA). In all cases, the chemical shift values for ¹H spectra are reported in ppm (δ) relative to residual CHD₂SO₂CD₃ (δ 2.50) or D₂O (δ 4.79), shift values for ¹³C spectra are reported in ppm (δ) relative to solvent peak dimethylsulfoxide-*d*₆ δ 39.43. Signals are quoted as s (singlet), d (doublet), t (triplet) and m (multiplet).

The mass spectra (MS, respectively, MSn) were measured on a LCQ FLEET ion trap and evaluated using Xcalibur v 2.5.0 software (both Thermo Fisher Scientific, San Jose, CA, USA). The sample was dissolved in deionized water (Goro, s.r.o., Prague, Czech Republic), and injected continuously (8 μ L/min) by using a Hamilton syringe into the electrospray ion source. The parameters of electrospray were set up as follows: sheath gas flow rate 20 arbitrary units, aux gas flow rate 5 arbitrary units, sweep gas flow rate 0 arbitrary units, spray voltage 5 kV, capillary temperature 275 °C, capillary voltage 13 V, tube lens 100 V.

6.2. Preparation of bisquaternary salts

Initially the monoquaternary semi-product was prepared: a solution of the 4-hydroxyiminomethylpyridine (4.0 g, 32.8 mmol) and 1,3-dibromopropane (16.7 mL, 163.8 mmol) in acetone (30 mL) was stirred at reflux for 8 h. The reaction mixture was cooled to room temperature and the crystalline crude product collected by filtration and washed with acetone (3 \times 20 mL). The solid crude product was recrystallized from MeCN (1 g of crude product per 100 mL of MeCN), where the boiling mixture was filtered under a reduced pressure. The filtrate was evaporated under a reduced pressure to produce the pure monoquaternary salt of 1-(3-bromopropyl)-4-hydroxyiminomethylpyridinium bromide (72%).⁴⁸

Secondly, the synthesis of the bisquaternary salt was completed. A solution of the monoquaternary salt (0.50 g, 1.5 mmol) and selected heteroaromatic compound (0.38 g, 3.0 mmol) in DMF (10 mL) was stirred at 70–80 °C for 8 h. The reaction mixture was cooled to room temperature and portioned with acetone (80 mL); the crystalline crude product was collected by filtration, washed with acetone (3 \times 20 mL) and recrystallized from

boiling MeCN. The pure bisquaternary salt was obtained as the solid compound insoluble in boiling MeCN.⁴⁸

6.3. Prepared bisquaternary salts

6.3.1. 4-Hydroxyiminomethyl-1,1'-(prop-1,3-diyl)-bispyridinium dibromide (8)

Mp 241–243 °C. Yield 80%. ¹H NMR and ¹³C NMR results are consistent with literature data.⁴⁶ ESI-MS: *m/z* 121.6 [M²⁺/2] (calcd for C₁₄H₁₇N₃O²⁺/2: 121.57). EA: calcd C, 41.71; H, 4.25; N, 10.42. Found: C, 41.75; H, 4.22; N, 10.07.

6.3.2. 4-Hydroxyiminomethyl-1,1'-(prop-1,3-diyl)-1-pyridinium-1'-pyridazinium dibromide (9)

Mp 247–249 °C. Yield 92%. ¹H NMR (300 MHz, DMSO-*d*₆): δ (ppm) 9.86 (d, 1H, *J* = 5.9 Hz, H-6'), 9.44 (d, 1H, *J* = 4.8 Hz, H-3'), 8.91 (d, 2H, *J* = 6.0 Hz, H-2,6), 8.58 (m, 1H, H-5'), 8.44 (m, 1H, H-4'), 8.24 (s, 1H, –CH=NOH), 8.05 (d, 2H, *J* = 6.3 Hz, H-3,5), 4.75 (t, 2H, *J* = 6.7 Hz, N'-CH₂-), 4.56 (t, 2H, *J* = 7.27 Hz, N-CH₂-), 2.27 (m, 2H, N-CH₂-CH₂-). ¹³C NMR (75 MHz, DMSO-*d*₆): δ (ppm) 154.47, 150.45, 148.50, 145.16, 145.06, 136.78, 136.15, 124.08, 61.02, 56.86. ESI-MS: *m/z* 243.1 [M–H⁺] (calcd for C₁₃H₁₆N₄O²⁺: 244.13). EA: calcd C, 38.64; H, 3.99; N, 13.86. Found: C, 38.47; H, 4.12; N, 14.02.

6.3.3. 4-Hydroxyiminomethyl-1,1'-(prop-1,3-diyl)-1-pyridinium-1'-quinolinium dibromide (10)

Mp 210–212 °C. Yield 57%. ¹H NMR (300 MHz, DMSO-*d*₆): δ (ppm) 9.70 (d, 1H, *J* = 5.9 Hz, H-2'), 9.38 (d, 1H, *J* = 8.4 Hz, H-4'), 9.02 (d, 2H, *J* = 6.0 Hz, H-2,6), 8.56 (m, 2H, H-3',8'), 8.45 (s, 1H, –CH=NOH), 8.30–8.21 (m, 4H, H-3,5,5',7'), 8.06 (m, 1H, H-6'), 6.39 (m, 1H, N'-CH₂-CH₂-), 6.12 (m, 1H, N-CH₂-CH₂-), 5.87 (d, 2H, *J* = 5.1 Hz, N'-CH₂-), 5.31 (d, 2H, *J* = 6.3 Hz, N-CH₂-). ¹³C NMR (75 MHz, DMSO-*d*₆): δ (ppm) 149.96, 148.60, 147.85, 144.95, 137.50, 135.63, 130.63, 129.88, 129.61, 128.31, 123.95, 122.31, 119.18, 60.29, 57.58. ESI-MS: *m/z* 146.6 [M²⁺/2] (calcd for C₁₈H₁₉N₃O²⁺/2: 146.58). EA: calcd C, 47.71; H, 4.23; N, 9.27. Found: C, 47.66; H, 4.27; N, 9.12.

6.3.4. 4-Hydroxyiminomethyl-1,1'-(prop-1,3-diyl)-1-pyridinium-1'-isoquinolinium dibromide (11)

Mp 227–229 °C. Yield 75%. ¹H NMR (300 MHz, DMSO-*d*₆): δ (ppm) 10.25 (s, 1H, H-1'), 9.11 (d, 2H, *J* = 6.6 Hz, H-2,6), 8.82 (d, 1H, *J* = 6.6 Hz, H-3'), 8.65 (d, 1H, *J* = 7.0 Hz, H-4'), 8.57 (d, 1H, *J* = 8.2 Hz, H-8'), 8.47 (s, 1H, –CH=NOH), 8.39 (d, 1H, *J* = 8.1 Hz, H-5'), 8.32–8.24 (m, 3H, H-3,5,7'), 8.09 (m, 1H, H-6'), 6.30 (m, 2H, N-CH₂-), 5.52 (m, 2H, N'-CH₂-), 5.40 (m, 2H, N-CH₂-CH₂-). ¹³C NMR (75 MHz, DMSO-*d*₆): δ (ppm) 150.20, 148.62, 145.11, 136.98, 134.86, 131.13, 130.44, 130.19, 129.96, 127.21, 127.11, 125.80, 123.99, 60.89, 60.31. ESI-MS: *m/z* 146.6 [M²⁺/2] (calcd for C₁₈H₁₉N₃O²⁺/2: 146.58). EA: calcd C, 47.71; H, 4.23; N, 9.27. Found: C, 47.77; H, 4.24; N, 9.02.

6.3.5. 4-Hydroxyiminomethyl-4'-methyl-1,1'-(prop-1,3-diyl)-bispyridinium dibromide (12)

Mp 236–238 °C. Yield 53%. ¹H NMR (300 MHz, DMSO-*d*₆): δ (ppm) 8.98 (d, 2H, *J* = 6.2 Hz, H-2,6), 8.88 (d, 2H, *J* = 6.0 Hz, H-2',6'), 8.32 (s, 1H, –CH=NOH), 8.13 (d, 2H, *J* = 6.2 Hz, H-3,5), 7.89 (d, 2H, *J* = 6.0 Hz, H-3',5'), 4.81–4.66 (m, 4H, N-CH₂-, N'-CH₂-), 2.56–2.48 (m, 2H, N-CH₂-CH₂-), 2.47 (s, 3H, –CH₃). ¹³C NMR (75 MHz, DMSO-*d*₆): δ (ppm) 159.04, 148.50, 145.12, 145.03, 143.84, 128.35, 124.04, 56.90, 56.48, 21.35. ESI-MS: *m/z* 128.6 [M²⁺/2] (calcd for C₁₅H₁₉N₃O²⁺/2: 128.58). EA: calcd C, 43.19; H, 4.59; N, 10.07. Found: C, 43.05; H, 4.72; N, 10.06.

6.3.6. 4-Hydroxyiminomethyl-4'-(1,1-dimethylethyl)-1,1'-(prop-1,3-diyl)-bispyridinium dibromide (13)

Mp 98–100 °C. Yield 17%. ¹H NMR (300 MHz, DMSO-*d*₆): δ (ppm) 9.13 (d, 2H, *J* = 6.2 Hz, H-2,6), 9.07 (d, 2H, *J* = 6.2 Hz, H-2',6'), 8.47 (s, 1H, –CH=NOH), 8.27 (d, 2H, *J* = 6.2 Hz, H-3,5), 8.21 (d, 2H, *J* = 6.2 Hz, H-3',5'), 4.81–4.69 (m, 4H, N–CH₂–, N'–CH₂–), 2.74–2.59 (m, 2H, N–CH₂–CH₂–), 1.36 (s, 9H, –CH₃). ¹³C NMR (75 MHz, DMSO-*d*₆): δ (ppm) 148.49, 145.13, 145.02, 144.22, 125.05, 124.03, 57.04, 56.44, 36.23, 29.46. ESI-MS: *m/z* 149.5 [M²⁺/2] (calculated for C₁₈H₂₅N₃O²⁺/2: 149.60). EA: calcd C, 47.08; H, 5.49; N, 9.15. Found: C, 46.95; H, 5.64; N, 9.25.

6.3.7. 4-Hydroxyiminomethyl-4'-phenyl-1,1'-(prop-1,3-diyl)-bispyridinium dibromide (14)

Mp 238–240 °C. Yield 30%. ¹H NMR (300 MHz, DMSO-*d*₆): δ (ppm) 9.00 (d, 2H, *J* = 6.2 Hz, H-2',6'), 8.95 (d, 2H, *J* = 6.2 Hz, H-2,6), 8.39 (d, 2H, *J* = 6.2 Hz, H-3',5'), 8.27 (s, 1H, –CH=NOH), 8.08 (d, 2H, *J* = 6.0 Hz, H-3,5), 7.91 (m, 2H, Ph), 7.46 (m, 3H, Ph), 4.58 (t, 4H, *J* = 7.0 Hz, N–CH₂–, N'–CH₂–), 2.29 (m, 2H, N–CH₂–CH₂–). ¹³C NMR (75 MHz, DMSO-*d*₆): δ (ppm) 155.07, 148.78, 145.42, 145.30, 145.20, 133.67, 132.41, 129.90, 128.36, 124.75, 124.33, 57.23, 56.73. ESI-MS: *m/z* 159.6 [M²⁺/2] (calcd for C₂₀H₂₁N₃O²⁺/2: 159.58). EA: calcd C, 50.13; H, 4.42; N, 8.77. Found: C, 49.99; H, 4.68; N, 8.68.

6.3.8. 4-Hydroxyiminomethyl-4'-hydroxymethyl-1,1'-(prop-1,3-diyl)-bispyridinium dibromide (15)

Mp 176–178 °C. Yield 76%. ¹H NMR (300 MHz, DMSO-*d*₆): δ (ppm) 9.06 (d, 2H, *J* = 6.2 Hz, H-2',6'), 9.02 (d, 2H, *J* = 6.2 Hz, H-2,6), 8.47 (s, 1H, –CH=NOH), 8.27 (d, 2H, *J* = 6.2 Hz, H-3',5'), 8.07 (d, 2H, *J* = 5.9 Hz, H-3,5), 6.21 (s, 2H, –CH₂–OH), 5.39–5.31 (m, 4H, N–CH₂–, N'–CH₂–), 4.86–4.69 (m, 2H, N–CH₂–CH₂–). ¹³C NMR (75 MHz, DMSO-*d*₆): δ (ppm) 148.64, 148.50, 145.08, 144.13, 130.14, 129.98, 124.33, 61.08, 60.26. ESI-MS: *m/z* 272.1 [M²⁺–H] (calcd for C₁₅H₁₉N₃O₂²⁺–H: 272.15). EA: calcd C, 41.59; H, 4.42; N, 9.70. Found: C, 41.43; H, 4.68; N, 9.54.

6.3.9. 4-Hydroxyiminomethyl-4'-methylcarbonyl-1,1'-(prop-1,3-diyl)-bispyridinium dibromide (16)

Mp 201–203 °C. Yield 53%. ¹H NMR (300 MHz, DMSO-*d*₆): δ (ppm) 9.35 (d, 2H, *J* = 6.2 Hz, H-2',6'), 9.08 (d, 2H, *J* = 6.2 Hz, H-2,6), 8.53 (d, 2H, *J* = 6.2 Hz, H-3',5'), 8.47 (s, 1H, –CH=NOH), 8.28 (d, 2H, *J* = 6.0 Hz, H-3,5), 6.34–6.16 (m, 2H, N–CH₂–CH₂–), 5.51–5.45 (m, 2H, N'–CH₂–), 5.40–5.34 (m, 2H, N–CH₂–), 2.76 (s, 3H, –CH₃). ¹³C NMR (75 MHz, DMSO-*d*₆): δ (ppm) 195.67, 148.65, 146.39, 145.09, 130.55, 129.69, 125.91, 124.02, 60.92, 60.21, 27.49. ESI-MS: *m/z* 285.0 [M²⁺] (calcd for C₁₆H₁₉N₃O₂²⁺: 285.15). EA: calcd C, 43.17; H, 4.30; N, 9.44. Found: C, 43.42; H, 4.28; N, 9.18.

6.3.10. 4'-Carboxy-4-hydroxyiminomethyl-1,1'-(prop-1,3-diyl)-bispyridinium dibromide (17)

Mp 230–232 °C. Yield 30%. ¹H NMR (300 MHz, D₂O-*d*₆): δ (ppm) 9.06 (d, 2H, *J* = 6.2 Hz, H-2,6), 8.88 (d, 2H, *J* = 6.2 Hz, H-2',6'), 8.44 (d, 2H, *J* = 6.2 Hz, H-3,5), 8.36 (s, 1H, –CH=NOH), 8.22 (d, 2H, *J* = 6.0 Hz, H-3',5'), 4.92–4.84 (m, 2H, N'–CH₂–), 4.61 (t, *J* = 5.6 Hz, N–CH₂–), 2.91–2.75 (m, 2H, N'–CH₂–CH₂–). ¹³C NMR (75 MHz, D₂O-*d*₆): δ (ppm) 216.02, 166.94, 149.90, 146.80, 146.19, 145.28, 128.45, 125.79, 58.91, 58.29. ESI-MS: *m/z* 143.5 [M²⁺] (calcd for C₁₅H₁₇N₃O₃²⁺: 143.57). EA: calcd C, 40.29; H, 3.83; N, 9.40. Found: C, 39.91; H, 4.17; N, 9.45.

6.3.11. 4-Ethylcarboxy-4'-hydroxyiminomethyl-1,1'-(prop-1,3-diyl)-bispyridinium dibromide (18)

Mp 163–165 °C. Yield 17%. ¹H NMR (300 MHz, DMSO-*d*₆): δ (ppm) 9.33 (d, 2H, *J* = 6.2 Hz, H-2,6), 9.08 (d, 2H, *J* = 6.2 Hz,

H-2',6'), 8.54 (d, 2H, *J* = 6.2 Hz, H-3,5), 8.47 (s, 1H, –CH=NOH), 8.27 (d, 2H, *J* = 6.0 Hz, H-3',5'), 6.33–6.15 (m, 2H, N–CH₂–CH₂–), 5.54–5.45 (m, 2H, N'–CH₂–), 5.42–5.30 (m, 2H, N'–CH₂–), 4.45 (q, 2H, *J*₁₂ = *J*₂₂ = 7.0 Hz, COO–CH₂–), 1.37 (t, 3H, *J* = 7.0 Hz, –CH₃). ¹³C NMR (75 MHz, DMSO-*d*₆): δ (ppm) 161.95, 148.64, 146.41, 145.09, 130.47, 129.73, 127.16, 124.01, 62.92, 61.11, 60.22, 13.81. ESI-MS: *m/z* 314.0 [M²⁺–H] (calcd for C₁₇H₂₁N₃O₃²⁺–H: 314.16). EA: calcd C, 42.97; H, 4.45; N, 8.84. Found: C, 43.36; H, 4.30; N, 8.85.

6.3.12. 4-Carbonitril-4'-hydroxyiminomethyl-1,1'-(prop-1,3-diyl)-bispyridinium dibromide (19)

Mp 216–218 °C. Yield 84%. ¹H NMR, ¹³C NMR, ESI-MS and EA results are consistent with the literature data.²⁸

6.3.13. 4-(1-Amino-1-hydroxyiminomethyl)-4'-hydroxyiminomethyl-1,1'-(prop-1,3-diyl)-bispyridinium dibromide (20)

Mp 147–149 °C. Yield 62%. ¹H NMR (300 MHz, DMSO-*d*₆): δ (ppm) 8.97 (m, 4H, H-2,2',6,6'), 8.30 (s, 1H, –CH=NOH), 8.19 (d, 2H, *J* = 6.2 Hz, H-3',5'), 8.12 (d, 2H, *J* = 6.2 Hz, H-3,5), 6.31 (s, 2H, –NH₂), 4.58 (t, 4H, *J* = 6.4 Hz, N–CH₂–, N'–CH₂–), 2.34 (m, 2H, N–CH₂–CH₂–). ¹³C NMR (75 MHz, DMSO-*d*₆): δ (ppm) 148.52, 147.95, 146.93, 145.14, 145.05, 144.69, 124.08, 122.75, 56.88, 56.73. ESI-MS: *m/z* 150.6 [M²⁺/2] (calcd for C₁₅H₁₉N₃O₂²⁺/2: 150.58). EA: calcd C, 39.07; H, 4.15; N, 15.19. Found: C, 39.50; H, 4.35; N, 15.05.

6.3.14. 3,4-Dicarbamoyl-4'-hydroxyiminomethyl-1,1'-(prop-1,3-diyl)-bispyridinium dibromide (21)

Mp 142–144 °C. Yield 44%. ¹H NMR (300 MHz, DMSO-*d*₆): δ (ppm) 9.18 (s, 1H, H-2), 9.09 (d, 1H, *J* = 6.4 Hz, H-6), 8.91 (d, 2H, *J* = 6.4 Hz, H-2',6'), 8.24 (s, 1H, –CH=NOH), 8.13 (m, 2H, 3-NH₂), 8.06 (d, 2H, *J* = 6.2 Hz, H-3',5'), 8.00 (d, 1H, *J* = 6.2 Hz, H-5), 7.88 (s, 2H, 4-NH₂), 4.55 (m, 4H, N–CH₂–, N'–CH₂–), 2.26 (m, 2H, N–CH₂–CH₂–). ¹³C NMR (75 MHz, DMSO-*d*₆): δ (ppm) 165.40, 163.68, 150.64, 148.57, 146.39, 145.18, 145.07, 144.55, 134.10, 126.13, 124.08, 57.53, 56.92. ESI-MS: *m/z* 164.6 [M²⁺/2] (calcd for C₁₆H₁₉N₅O₃²⁺/2: 164.58). EA: calcd C, 39.29; H, 3.92; N, 14.32. Found: C, 39.45; H, 3.98; N, 14.18.

6.4. In vitro reactivation assay

The reactivation ability was measured on a multichannel spectrophotometer Sunrise (Tecan, Salzburg, Austria). The previously used Ellman's procedure was slightly adapted.²⁹ Standard polystyrene microplates with 96 wells (Nunc, Rockville, Denmark) were chosen as reaction cuvettes. Recombinant hAChE (Sigma–Aldrich) was used throughout experiments. Tabun (GA; O-ethyl-N,N-dimethylphosphoramidocyanidate) was obtained from the Military Facility in Brno. Pesticides paraoxon (POX), methylparaoxon (MePOX) and diisopropylfluorophosphate (DFP) were purchased from (Sigma–Aldrich). 50 mM phosphate buffer pH 7.4 was used throughout all experiments.

The activity of the enzyme was adjusted to 0.002 U/μl. Inhibited enzyme was prepared directly before the testing of the potential reactivator. Phosphate buffer containing 1 mg/ml albumin, and a solution of enzyme (15 μl) was incubated with 1 μM GA or 10 μM POX or 10 μM MePOX or 100 μM DFP (5 μl) at room temperature to achieve 95% inhibition. The time of inhibition was selected with respect to the inhibition half-life of each inhibitor (GA–40 min, POX and MePOX–1 h, DFP–1 h 20 min).

One well was filled by the following chemicals–inhibited enzyme solution (20 μl), phosphate buffer (60 μl), 0.4 mg/ml 5,5'-dithio-bis-(2-nitrobenzoic)-acid (DTBN; 20 μl). Cholinesterase was reactivated by the addition of 100 μM or 10 μM oxime-reactivator dissolved in the phosphate buffer. Enzyme activity

was measured after a 15 min incubation via addition of 1 mM acetylthiocholine chloride (20 μ l, ATChCl). Oximolysis was determined similarly by displacing enzyme with the phosphate buffer containing 1 mg/ml albumin. The microplate was gently shaken by the incorporated robotic system just before measurement. Absorbance was measured against phosphate buffer at 412 nm.

The reactivation ability was calculated according the subsequent equation.

$$(\%) = \frac{A_r - A_{ox}}{A_0 - A_i} \times 100$$

A_r indicates absorbance at 412 nm provided by cholinesterase reactivated by reactivator; A_{ox} —absorbance provided by oximolysis; A_0 —absorbance provided by intact cholinesterase; A_i —absorbance provided by inhibited cholinesterase.

All measurements were made in triplicate and the reactivation data were expressed as average value \pm standard deviation (SD).

6.5. In vitro inhibition assay

The multichannel spectrophotometer Sunrise (Tecan, Salzburg, Austria) was used for all measurements of hAChE activity. The previously optimized Ellman's procedure was slightly adapted in order to estimate inhibitory properties hAChE reactivators.²⁹ 96-wells photometric microplates made from polystyrene (Nunc, Rockilde, Denmark) were used for measuring purposes. Recombinant hAChE (Aldrich; commercially purified by affinity chromatography) was suspended in phosphate buffer (pH 7.4) to a final activity of 0.002 U/ μ l. Cholinesterase (5 μ l), a freshly mixed solution of 0.4 mg/ml 5,5'-dithio-bis(2-nitrobenzoic) acid (40 μ l), 1 mM acetylthiocholine chloride in phosphate buffer (20 μ l) and the appropriate concentration of inhibitor (1 mM–0.1 nM; 5 μ l) were injected per well. Absorbance was measured at 412 nm after 5 min incubation using automatic shaking of the microplate.

Percentage of inhibition (I) was calculated from the measured data as follows:

$$I = 1 - \frac{\Delta A_i}{\Delta A_0}$$

ΔA_i indicates absorbance change provided by cholinesterase exposed to anticholinergic compound. ΔA_0 indicates absorbance change caused by intact cholinesterase, where phosphate buffer was applied in the same way as the anticholinergic compound.

IC_{50} was determined using Origin 6.1 (Northampton, MA, USA). Percentage of inhibition was calculated by Hill plot ($n = 1$). The other plot variants (between -2 and $+2$) were not optimal and the coefficient of determination was lower compared to chosen method. Subsequently, IC_{50} was computed.

6.6. Molecular docking

Docking calculations were carried out using Autodock 4.0.1.⁴⁹ A Lamarckian genetic algorithm (Amber force field) was used. A population of 150 individuals and 2500000 function evaluations were applied. The structure optimization was performed for 27000 generations. Electrostatic energies were calculated for all non-bonds between moving atoms. Minimum electrostatic potential (-41.82 kcal/mol) and maximum electrostatic potential (40.09 kcal/mol) were set up. Docking calculations were set to 50 runs. At the end of calculation, Autodock performed cluster analysis.

The structure of *Mus musculus* GA-AChE and human GA-AChE were prepared from the crystal structure (pdb code 2jez, 2jf0 and 1b41) using Autodock Tools 1.5.2.^{35,36,49} The conserved water molecules were identified by comparing various crystal structures containing tabun-inhibited AChE in Relibase.⁵⁰ The 3D affinity grid box was designed to include the full active and peripheral site of

AChE. The number of grid points in the x-, y- and z-axes was 110, 110 and 110 with grid points separated by 0.253 Å. The O-ethyl group of GA was set up as flexible moiety. The molecular model of ligand was built using ChemDraw 11.1 and minimized with UCSF Chimera 1.3 (Amber Force field) in charged form.⁵¹ The maximum root mean square tolerance for conformational cluster analysis was 2.0 Å. The visualization of enzyme-ligand interactions (Fig. 5) was prepared using Pymol 1.1.⁵²

Acknowledgements

The work was supported by the Grant Agency of Ministry of Education, Youth and Sports Czech Republic (ME09086) and by the grant SVV-2010-261-001. F.G.M. is funded by the Alzheimer's Research Trust, UK.

References and notes

- Marrs, T. C. *Pharmacol. Therap.* **1993**, *58*, 51.
- Gupta, R. *Toxicology of Organophosphate & Carbamate Compounds*; Elsevier Academic Press: London, 2006, pp 5–69.
- Clothier, B.; Johnson, M. K. *Biochem. J.* **1980**, *185*, 739.
- Bajgar, J. *Adv. Clin. Chem.* **2004**, *38*, 151.
- Newmark, J. *Arch. Neurol.* **2004**, *61*, 649.
- Bajgar, J.; Fusek, J.; Kassa, J.; Kuca, K.; Jun, D. *Curr. Med. Chem.* **2009**, *16*, 2977.
- Stojiljkovic, M. P.; Jokanovic, M. *Arh. Hig. Rada Toksikol.* **2006**, *57*, 435.
- Carletti, E.; Li, H.; Li, B.; Ekstrom, F.; Nicolet, Y.; Loiodice, M.; Gillon, E.; Froment, M. T.; Lockridge, O.; Schopfer, L. M.; Masson, P.; Nachon, F. *J. Am. Chem. Soc.* **2008**, *130*, 16011.
- Kuca, K.; Jun, D.; Musilek, K. *Mini-Rev. Med. Chem.* **2006**, *6*, 269.
- Kuca, K.; Jun, D.; Bajgar, J. *Drug Chem. Toxicol.* **2007**, *30*, 31.
- Kuca, K.; Musilek, K.; Stodulka, P.; Marek, J.; Hanusova, P.; Jun, D.; Hrabanova, M.; Kassa, J.; Dolezal, B. *Lett. Drug Des. Discovery* **2007**, *4*, 510.
- Worek, F.; Thiermann, H.; Szinicz, L.; Eyer, P. *Biochem. Pharmacol.* **2004**, *68*, 2237.
- Buckley, N. A.; Roberts, D.; Eddleston, M. *Br. Med. J.* **2004**, *329*, 1231.
- Musilek, K.; Dolezal, M.; Gunn-Moore, F.; Kuca, K. *Med. Res. Rev.* **2010**, doi:10.1002/med.20192.
- Kuca, K.; Musilek, K.; Jun, D.; Pohanka, M.; Ghosh, K. K.; Hrabanova, M. *J. Enzyme Inhib. Med. Chem.* **2010**, *25*, 509.
- Berend, S.; Vrdoljak, A. L.; Radić, B.; Kuca, K. *Chem. Biol. Interact.* **2008**, *175*, 413.
- Kuca, K.; Cabal, J.; Musilek, K.; Jun, D.; Bajgar, J. *J. Appl. Toxicol.* **2005**, *25*, 491.
- Musilek, K.; Jun, D.; Cabal, J.; Kassa, J.; Gunn-Moore, F.; Kuca, K. *J. Med. Chem.* **2007**, *50*, 5514.
- Kassa, J.; Karasova, J.; Musilek, K.; Kuca, K. *Toxicology* **2008**, *243*, 311.
- Kassa, J.; Karasova, J. Z.; Pavlikova, R.; Misik, J.; Caisberger, F.; Bajgar, J. *J. Appl. Toxicol.* **2010**, *30*, 120.
- Kovarik, Z.; Lucic Vrdoljak, A.; Berend, S.; Catalinic, M.; Kuca, K.; Musilek, K.; Radić, B. *Arh. Hig. Rada Toksikol.* **2009**, *60*, 19.
- Lorke, D. E.; Hasan, M. Y.; Arafat, K.; Kuca, K.; Musilek, K.; Schmitt, A.; Petroianu, G. A. *J. Appl. Toxicol.* **2008**, *28*, 422.
- Lorke, D. E.; Nurulain, S. M.; Hasan, M. Y.; Kuca, K.; Musilek, K.; Petroianu, G. A. *J. Appl. Toxicol.* **2008**, *28*, 920.
- Kuca, K.; Cabal, J.; Jun, D.; Musilek, K. *Neurotox. Res.* **2007**, *11*, 101.
- Nurulain, S. M.; Lorke, D. E.; Hasan, M. Y.; Shafullah, M.; Kuca, K.; Musilek, K.; Petroianu, G. A. *Neurotox. Res.* **2009**, *16*, 60.
- Musilek, K.; Holas, O.; Jun, D.; Dohnal, V.; Gunn-Moore, F.; Opletalova, V.; Dolezal, M.; Kuca, K. *Bioorg. Med. Chem.* **2007**, *15*, 6733.
- Musilek, K.; Holas, O.; Misik, J.; Pohanka, M.; Novotny, L.; Dohnal, V.; Opletalova, V.; Kuca, K. *ChemMedChem* **2010**, *5*, 247.
- Musilek, K.; Holas, O.; Kuca, K.; Jun, D.; Dohnal, V.; Dolezal, M. *Bioorg. Med. Chem. Lett.* **2006**, *16*, 5673.
- Pohanka, M.; Jun, D.; Kuca, K. *Talanta* **2008**, *77*, 451.
- Kovarik, Z.; Calic, M.; Sinko, G.; Bosak, A.; Berend, S.; Vrdoljak, A. L.; Radić, B. *Chem. Biol. Interact.* **2008**, *175*, 173.
- Tattersall, J. E. H. *Brit. J. Pharmacol.* **1993**, *108*, 1006.
- Musilek, K.; Kuca, K.; Jun, D.; Dohnal, V.; Dolezal, M. *J. Enzyme Inhib. Med. Chem.* **2005**, *20*, 409.
- Musilek, K.; Holas, O.; Kuca, K.; Jun, D.; Dohnal, V.; Dolezal, M. *J. Enzyme Inhib. Med. Chem.* **2007**, *22*, 425.
- Sinko, G.; Brglez, J.; Kovarik, Z. *Chem. Biol. Interact.* **2010**, *187*, 172.
- Kryger, G.; Harel, M.; Giles, K.; Tokar, L.; Velan, B.; Lazar, A.; Kronman, C.; Barak, D.; Ariel, N.; Shafferman, A.; Silman, I.; Sussman, J. L. *Acta Crystallogr., Sect. D* **2000**, *56*, 1385.
- Ekstrom, F. J.; Astot, C.; Pang, Y. P. *Clin. Pharmacol. Ther.* **2007**, *82*, 282.
- Ekstrom, F.; Akfur, C.; Tunemalm, A.-K.; Lundberg, S. *Biochemistry* **2006**, *45*, 74.
- Hornberg, A.; Artursson, E.; Warme, R.; Pang, Y. P.; Ekstrom, F. *Biochem. Pharmacol.* **2010**, *79*, 507.
- Ekstrom, F.; Hornberg, A.; Artursson, E.; Hammarstrom, L.-G.; Schneider, G.; Pang, Y.-P., not cited on www.pdb.org.

40. Carletti, E.; Colletier, J. P.; Dupeux, F.; Trovaslet, M.; Masson, P.; Nachon, F. *J. Med. Chem.* **2010**, 53, 4002.
41. Dvir, H.; Silman, I.; Harel, M.; Rosenberry, T. L.; Sussman, J. L. *Chem. Biol. Interact.* **2010**, 187, 10.
42. Giacobini, E. In *Cholinesterases and Cholinesterase Inhibitors*; Giacobini, E., Ed.; Martin Dunitz: London, 2000; pp 1–226.
43. Bedford, C. D.; Miura, M.; Bottaro, J. C.; Howd, R. A.; Nolen, H. W. *J. Med. Chem.* **1986**, 29, 1689.
44. Musilek, K.; Holas, O.; Kuca, K.; Jun, D.; Dohnal, V.; Opletalova, V.; Dolezal, M. *J. Enzym. Inhib. Med. Chem.* **2008**, 23, 70.
45. De Jong, L. P. A.; Benschop, H. P.; Vandenberg, G. R.; Wolring, G. Z.; Dekorte, D. C. *Eur. J. Med. Chem.* **1981**, 16, 257.
46. Kuca, K.; Musilek, K.; Paar, M.; Jun, D.; Stodulka, P.; Hrabínova, M.; Marek, J. *Molecules* **2007**, 12, 1964.
47. Ma, J. C.; Dougherty, D. A. *Chem. Rev.* **1997**, 97, 1303.
48. Musilek, K.; Kuca, K.; Jun, D.; Dolezal, M. *Lett. Org. Chem.* **2006**, 3, 831.
49. Morris, G. M.; Goodsell, D. S.; Halliday, R. S.; Huey, R.; Hart, W. E.; Belew, R. K.; Olson, A. J. *J. Comput. Chem.* **1998**, 19, 1639.
50. Available on http://www.ccdc.cam.ac.uk/free_services/relibase_free/.
51. Pettersen, E. F.; Goddard, T. D.; Huang, C. C.; Couch, G. S.; Greenblatt, D. M.; Meng, E. C.; Ferrin, T. E. *J. Comput. Chem.* **2004**, 25, 1605.
52. DeLano, W. L. The PyMOL Molecular Graphics System, 2002. On the World Wide Web <http://www.pymol.org>.